Spectral Profiling for the Simultaneous Observation of Four Distinct Fluorescent Proteins and Detection of Protein-Protein Interaction via Fluorescence Resonance Energy Transfer in Tobacco Leaf Nuclei[1]

Naohiro Kato, Dominique Pontier[2], and Eric Lam*

Biotech Center, Rutgers University, 59 Dudley Road, New Brunswick, New Jersey 08901–8520

The control of subcellular localization of proteins and their interaction with other partners in vivo are important parameters that provide clues to their function and regulation. The ability to simultaneously track multiple protein species with high resolution should provide a valuable assay system to study and characterize various types of posttranslational control pathways. In this work, we established the system and a method involving "spectral profiling" for the resolution of four different fluorescent protein tags in the same viewing field using digital imaging technology. With these techniques, we have (a) developed new derivatives of mGFP5, which is commonly used in the plant field, that are about three times brighter; (b) demonstrated that four spectrally distinct fluorescent proteins (cyan, green, yellow, and red) that are fused to a transcription factor could be stably expressed in nuclei and distinguished in tobacco (*Nicotiana tabacum*) mesophyll cells; and (c) shown that interaction between partners of a dimeric transcription factor can be detected by measuring fluorescence resonance energy transfer. These technologies should help one to study protein-protein interactions efficiently, especially for nuclear proteins under in vivo conditions.

The green fluorescent protein (GFP) from jellyfish is widely used as a powerful tool in cell biology, serving as a vital reporter for monitoring localization and dynamics of proteins and organelles in living cells (Goodwin, 1999; Ikawa et al., 1999). GFP variants with shifted and enhanced excitation/emission characteristics (such as blue [BFP], cyan [CFP], and yellow [YFP] fluorescent derivatives of GFP) and new fluorescent proteins such as the red fluorescent protein from tropical corals (CLONTECH Laboratories, Palo Alto, CA) have been developed and offer enormous potential for multilabeling experiments and protein-protein interaction studies in vivo. These multilabeling experiments with fluorescent proteins have been thought to be unsuitable in plants using a conventional epifluorescence microscope due to crossovers in their excitation and emission spectra and high background signals from autofluorescence of chlorophyll, cell wall, and high concentrations of phenolic compounds in some cell types. Special equipment and methodology, such as fluorescence lifetime measurement, is required to resolve the GFP signals from background fluorescence (Pepperkok et al., 1999).

In this report, we have constructed enhanced variants of GFP, designated as ELGFP6 and ELGFP6.1, from mGFP5, which is a plant-optimized GFP variant that has been modified to remove the cryptic splice site as well as mutated for better temperature stability (Haseloff, 1999). In addition to improving mGFP5 by site-directed mutagenesis, we also expressed the humanized and spectrally enhanced GFP variants, enhanced blue fluorescent protein (EBFP), enhanced cyan fluorescent protein (ECFP), and enhanced yellow fluorescent protein (EYFP), as well as the new DsRed2 (CLONTECH Laboratories) in nuclei of tobacco (*Nicotiana tabacum*) mesophyll cells to perform multilabel imaging experiments with a conventional epifluorescence microscope. Our data suggest that DsRed2 and EYFP proteins could be more suitable than the other three fluorescent proteins for obtaining a clear image with high signal-to-background ratio (S/B) in nuclei. We demonstrate that ECFP, ELGFP6.1, EYFP, and DsRed2 can be distinguished with optimized filter conditions and a CCD camera in a single viewing frame. We also demonstrate the use of EYFP and ECFP to monitor protein-protein interactions between known transcription factors in the nucleus by fluorescence resonance energy transfer (FRET) analysis. These results demonstrate the feasibility of using these protein tags for studies involving nuclear proteins and their interaction in living plant cells using relatively accessible technologies.

[1] This work was supported by the Plant Genome Research Program of the National Science Foundation (grant nos. 9872636 and 0077167) and in part by the Charles and Johanna Busch Memorial Fund at Rutgers University (grant no. 6–49142).

[2] Present address: Laboratoire de Génétique Moléculaire des Plantes, Université J. Fourier et Centre National de la Recherche Scientifique (Unité Mixte de Recherche 5575), Boite Postale 53, 38041 Grenoble cedex 9, France.

* Corresponding author; e-mail Lam@aesop.rutgers.edu; fax 732–932–6535.

www.plantphysiol.org/cgi/doi/10.1104/pp.005496.

RESULTS AND DISCUSSION

Construction of Enhanced Fluorescent Protein Variants from the Plant-Optimized GFP mGFP5

Although the mGFP5 variant constructed by Haseloff et al. (1997) is widely used and allows for efficient GFP expression in plant cells, we seek to improve its brightness for better detection under lower expression level conditions. Haseloff et al. constructed a variant of mGFP5, mGFP6, by the introduction of two-point mutations (conversions of Phe-64 to Leu and Ser-65 to Thr, F64L, and S65T) to change the emission and the excitation characteristics of the protein (Haseloff, 1999). However, a detailed study of the fluorescence properties of mGFP6 has yet to be reported. In this work, we constructed a variant of mGFP5 by the introduction of point mutation(s) (sequential conversion of Ser-65 to Cys [S65C] and then Phe-64 to Leu [F64L and S65C]) because it was reported previously that conversions of F64L and S65C increase the fluorescence 1.5 to 3 times higher than conversions of F64L and S65T (Stauber et al., 1998). We designated these mGFP5 variants ELGFP6 (S65C) and ELGFP6.1 (F64L and S65C). The fluorescence spectra of purified bacteria expressing recombinant ELGFP6 protein showed excitation and emission maxima of 480 and 508 nm, respectively (Fig. 1A; Table I). To characterize the fluorescence intensity of ELGFP6 protein, we compared purified ELGFP6 and mGFP5 proteins (Fig. 1B) with a fluorescence spectrophotometer. Our comparison revealed that the relative fluorescence intensity of ELGFP6 at an excitation wavelength of 480 nm is at least 2.7 times higher than that of mGFP5 with an excitation maximum of 474 nm (Fig. 1B). ELGFP6.1 showed no significant difference from ELGFP6 in terms of fluorescence excitation and emission spectra and its relative fluorescence intensity. However, when we analyzed purified ELGFP6.1 by Coomassie Brilliant Blue-stained SDS-PAGE, we consistently observed two major bands that migrated closely together (data not shown). The cause of this size heterogeneity of recombinant ELGFP6.1 protein in the gel is unclear at present, although we speculate that it may be due to anomalous behavior of this particular GFP variant under SDS-PAGE conditions.

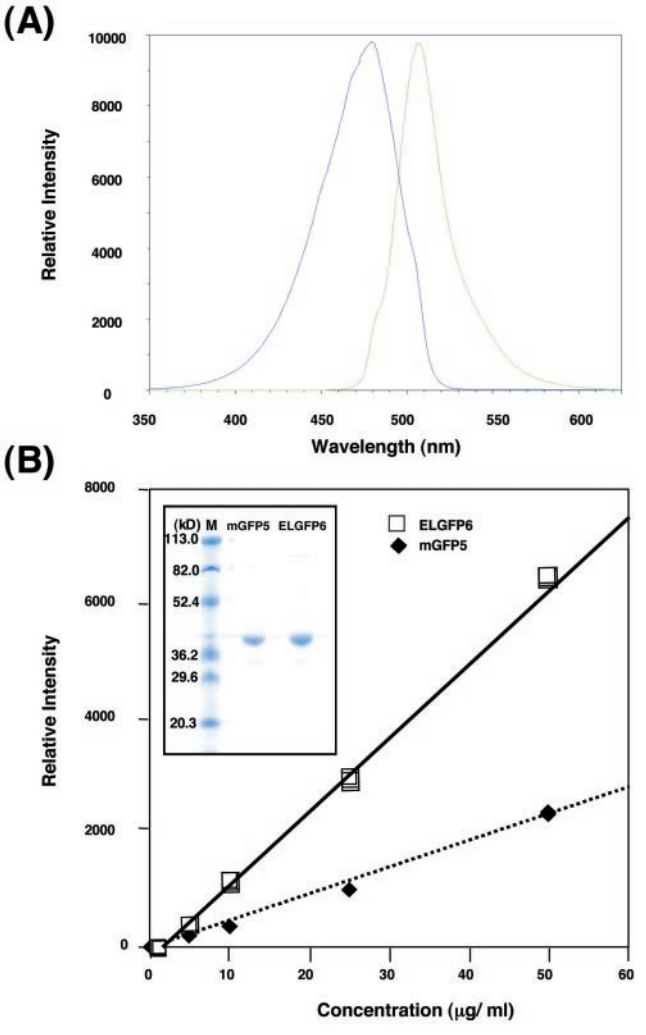

Figure 1. Spectral characteristics of an S65C mutant GFP variant derived from mGFP5. A, Fluorescence spectra of ELGFP6. Excitation and emission wavelength of 15 μg of purified bacteria expressing ELGFP6 protein in 1 mL of Tris (10 mM)-EDTA (10 mM) buffer, pH 8.0, was scanned at 508-nm emission maximum and 480-nm excitation maximum, respectively. Excitation scan curve (blue) and emission scan curve (green) were overlaid. B, Fluorescence intensity comparison between purified mGFP5 and ELGFP6. Ten micrograms of purified recombinant mGFP5 (Haseloff et al., 1997) and ELGFP6 (this study) was separated by SDS-PAGE and stained with Coomassie Brilliant Blue (inset). Different concentration series (10, 25, and 50 μg mL^{-1} in Tris [10 mM]-EDTA [10 mM] buffer, pH 8.0) of mGFP5 and ELGFP6 were subjected to quantitative analysis with a fluorescence spectrophotometer. Three independent measurements were plotted, and linear curve fits were drawn.

S/B Ratio of Fluorescent Proteins in Tobacco Leaves

A major limitation factor for epifluorescence microscopy is S/B because the images are created on a dark field. If the background signals are too high, the epifluorescence signals are covered by the background signals and it cannot be observed. In plants, chlorophylls and cell wall components are the major contributors of autofluorescence signals (Johnson et al., 2000; Smith, 2000) and posed significant barriers to the detection of fluorescent protein signals. Moreover, variant physiological status of plants may quantitatively affect the level of autofluorescence signals. Therefore, we have to consider the background problem associated with different excitation and emission filter conditions used for the various fluorescent proteins. We studied the S/B for each fluorescent protein under in vivo conditions to ascertain the optimal method for their detection in plant cells.

We used tobacco leaves as a model case with a conventional epifluorescence microscope equipped

Table I. *Protein spectral properties (nm) used in this study*

Spectral data of fluorescent proteins except ELGFP6 (6.1) were obtained from CLONTECH Laboratories. EXmax, Excitation max; EMmax, emission max. The nos. in parentheses indicate minor max wavelength.

Protein	EBFP		ECFP		ELGFP6 (6.1)		EYFP		DsRed2	
	EXmax	EMmax	EXmax	EMmax	EXmax	EMmax	EXmax	EMmax	EXmax	EMmax
	380	440	433 (453)	475 (501)	480	508	513	527	558	583

with a cooled CCD camera for detection. One of the advantages of the CCD camera for fluorescent analysis is that we can analyze the fluorescent signals in microscopy images without expensive equipment. First, we quantitated background signal contributions in tobacco leaves with the filter set optimized for each fluorescent protein excitation/emission spectra (Fig. 2). Ideally, we should not detect any fluorescence using these filter sets because no fluorescent proteins with these optical properties are expressed in plants. The signals detected using each filter set thus are considered as background signals. Relative values of background signals may vary with different microscopy setup because physical conditions such as electronic noise, spectral sensitivity of the CCD device, and optical properties of filters, fluorescent lamp, and objective lens are all important contributing factors. Under our conditions with the BFP filter set, we observed 10 times higher background signals than that with the YFP filter set, which showed the lowest value among filter sets that we examined, and the rhodamine (RD) filter set resulted in about 7 times higher background signals than that obtained with YFP filter set (Fig. 2).

We then measured S/B values for each autofluorescent protein in tobacco leaf cells. We expressed fluorescent proteins in nuclei that can be easily identified under the epifluorescence microscope when these proteins are produced. The nuclei are relatively large organelles (10–30 μm in the tobacco mesophyll cells) and can accumulate a large amount of proteins. Moreover, because nuclei contain relatively little autofluorescent materials, and are normally localized away from chloroplasts and cell walls, they are amenable to perform multicolor labeling experiment within tissues. To localize the fluorescent proteins in nuclei, we fused various fluorescent proteins (EBFP, ECFP, ELGFP6.1, EYFP, and DsRed2) to a plant transcription factor TGA5 so that the expressed proteins would accumulate in the nucleus. The TGA transcription factor family is one of the well-characterized basic Leu zipper proteins in plants, and is well known to form hetero- and homodimers in vitro and in vivo (Miao et al., 1994). We fused the Arabidopsis TGA5 coding region to the 3′ end of GFP variants and DsRed2. These fusion genes are then cloned downstream of the cauliflower mosaic virus 35S promoter in a binary vector, pEL103 (Mittler et al., 1995). To express the protein of interest in tobacco leaf cells, we used a transient expression assay with *Agrobacterium tumefaciens*, which was modified from a previously reported method (Yang et al., 2000). Under our conditions, we could detect the expressing fluorescent proteins in over 100 nuclei on the infiltrated area of tobacco mesophyll cells 4 d after infiltration. Therefore, this method provides a relatively simple, quick, and convenient analysis system.

Nuclei accumulating each fluorescent protein were observed with the filter set optimized for each fluorescent protein's excitation/emission characteristics. The signals in nuclei were then subtracted by the average background and divided by the average of background signals obtained from mock-treated plants. This calculation gave us the S/B values for each fluorescent protein in the tissues tested (Fig. 3A). The results showed that the S/B for EYFP is approximately 5, whereas the S/B for DsRed2 is approximately 4, and these two proteins exhibited the highest S/B values among the proteins tested. The observation that the S/B value of DsRed2 is approximately 2 times higher than that of EGFP6.1 suggests that DsRed2 could be useful addition to the enhanced YFP, GFP, and CFP as fluorescent tags for obtaining high S/B images of nuclei even for tissues where chlorophyll and other pigments are abundant. As we mentioned before, the relative values of S/B may vary with different microscope and instrument settings; thus, the precise S/B values for each of the fluorescent proteins may vary depending on the experimental setup. Because the YFP filter set showed low background signals in addition to a high S/B value, we suggest that EYFP may be an optimal fluorescent protein for obtaining high S/B images with nuclei of tobacco leaves. During this study, we

Table II. *Filter spectral properties (nm) used in this study*

Filter properties were obtained from Chroma Technology Corporation (Brattleboro, VT). EX, Excitation; EM, emission.

Filter	BFP		CFP		GFP		YFP		RD	
	EX	EM	EX	EM	EX	EM	EX	EM	EX	EM
	380/30	445/40	436/10	470/30	460/20	500/22	523/20 500/20[a]	568/50 535/30[a]	555/28	617/73

[a] Filters only used for FRET analysis.

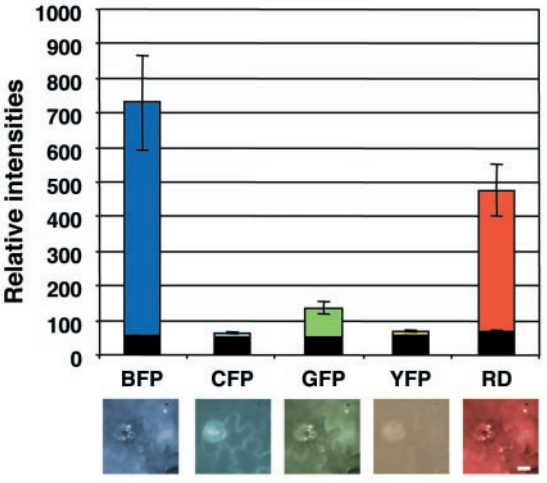

Figure 2. Comparison of background signals of tobacco leaves under different filter conditions. Autofluorescence of tobacco leaves with different filter conditions described at the bottom of each column were observed with an microscope equipped with 10× objective lens and cooled CCD camera that has a 12-bit (0–4,095) dynamic range. The columns show the average signal of 256- × 256-pixel areas from three independent experiments with SDS. The black portion in each column shows the noise signals that were obtained under identical conditions without a specimen on a microscope slide. Typical images obtained with a 60× lens are shown under each filter condition. Bar in the image = 20 μm.

realized that observing plants with the CFP filter set often caused the appearance of bubbles in leaf tissues that may result from the production of oxygen by PSII upon prolonged exposure to blue light. This finding suggests that it may be difficult to observe plant materials expressing ECFP proteins for a long time (i.e. 3 s) because formation of air bubbles will produce optical aberrations. We could not visualize EBFP-TGA5-accumulating nuclei in infiltrated tobacco leaves. This probably results from high background signals in leaf tissues as previously described because we could observe EBFP fusion proteins under identical conditions using a bacteria strain that expresses EBFP fusion protein (data not shown).

To confirm that similar levels of each protein are produced under our transient assay conditions, we performed western-blot analysis with antipolyclonal GFP antibodies (CLONTECH Laboratories) using crude protein extracts from the infiltrated tissues (Fig. 3B). The results suggested EBFP, ECFP, ELGFP6.1, and EYFP fusion proteins are all expressed to similar levels. Because the antibodies that we used do not cross-react with DsRed2 protein, we could not quantitate its expression level at this point.

Distinguishing a Fluorescent Protein from Other Fluorescent Proteins in a Single Viewing Frame

A major concern for multicolor epifluorescence microscopy is crossover between the spectra of the different emitters. Each fluorescent molecule has characteristic absorption and emission spectra. In theory, one can selectively detect fluorescence from a particular fluorescent protein of a mixture in a single viewing field by switching the filter combinations that are optimized according to the spectral maxima of each fluorescent material. However, because the slopes of the excitation and emission spectra for the various related fluorescent proteins can overlap to various extents, a fluorescence emitter can often be detected with filter sets that are designed for observing other spectrally distinct compounds. For example, Figure 4 shows representative transformed cells resulting from infiltration with each of the vectors. The transformed cells exhibited intense fluorescence in the nucleus when observed with filter sets optimized for the particular fluorescent proteins. However, one can clearly observe the nuclear images with one or more of the other filter sets that are optimized for different fluorescent proteins. For instance, with the construct expressing ELGFP6.1-TGA5, fluorescence was observed in a nucleus with the YFP filter set and CFP filter set as well as the GFP filter set. We refer to this phenomenon as "crossover" for simplicity.

When spectrally distinct fluorescent proteins accumulate in different locations in a single viewing frame, the crossover signals can interfere with the assignment of fluorescent signals to the appropriate

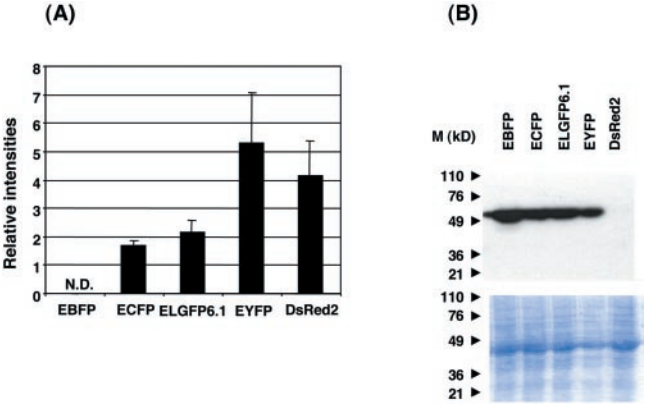

Figure 3. Comparison of S/B ratios for different fluorescent proteins expressed in leaf nuclei. A, Tobacco leaves expressing four different fluorescent proteins, which are individually fused to TGA5, were observed with a 10× objective lens. Nuclear fluorescence from three independent experiments (ECFP, 57 nuclei; ELGFP6.1, 65 nuclei; EYFP, 100 nuclei; and DsRed2, 54 nuclei) were averaged out per pixel, and then compared with the average of background signals that were collected separately (Fig. 2). The expressing fluorescent proteins are described on the bottom of each column as EBFP, ECFP, ELGFP6.1, EYFP, and DsRed2. N.D., Not determined. B, Confirmation that similar levels of protein are expressed with each construct. Proteins of *A. tumefaciens*-infiltrated tobacco leaves were extracted and subjected to western-blot assay using anti-GFP polyclonal antibodies. The sizes of the protein markers are shown on the left in kilodaltons. Lower, Coomassie Brilliant Blue dye-stained SDS polyacrylamide gel where similar amounts of proteins as for western blot were loaded.

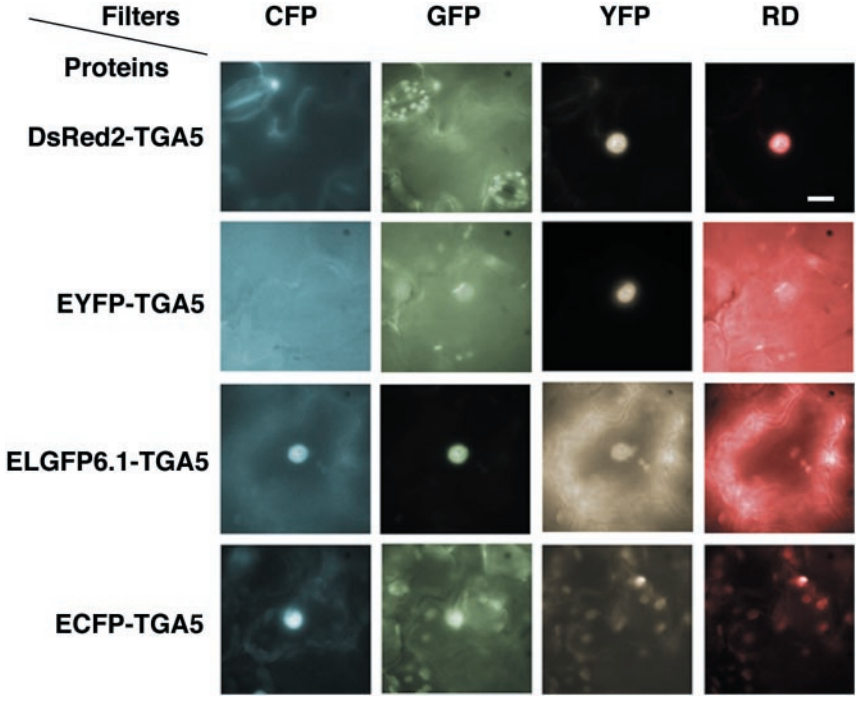

Figure 4. Observation of fluorescent protein expressed in tobacco leaf mesophyll cells. One- to 2-month-old tobacco leaves were infiltrated with *A. tumefaciens* with vectors expressing different fluorescent proteins fused to the N terminus of a transcription factor TGA5 under the cauliflower mosaic virus 35S promoter. Leaves were observed with an epifluorescence microscope equipped with a 60× water immersion objective lens 4 d after infiltration. The proteins accumulating in nuclei are indicated on the left. CFP, GFP, YFP, and RD on the top indicate the corresponding optical filter conditions (see Table II). Bar = 30 μm.

protein. However, because the crossover ratio is characteristic of the particular filter conditions for each fluorescent protein and it does not depend on signal intensity, we should be able to distinguish one fluorescent protein from the others in another location. Our strategy is that after we measure the crossover intensities for each fluorescent protein with each filter set, we will create the crossover intensity ratio profiles for each protein. Once we create the profiles for each protein, we should then be able to identify each nucleus that shows one of the profiles.

First, we measured the fluorescence intensities of four populations of nuclei, which express ECFP, ELGFP6.1, EYFP, or DsRed2, under each of the four optical filter conditions (CFP, GFP, YFP, or RD filter set). We then subtracted the averaged-background signals from the nucleus value. The remaining value then gives us the average crossover ratio of each filter set. ECFP-expressing nuclei show 0:0.08:0.11:1.00 (RD:YFP:GFP:CFP) intensity ratio for each filter set, respectively. ELGFP6.1-expressing nuclei show a ratio of 0:0.02:1:0.04 (RD:YFP:GFP:CFP). EYFP-expressing nuclei show 0:1:0:0 (RD:YFP:GFP:CFP). DsRed2-expressing nuclei show 1.00:0.09:0:0 (RD:YFP:GFP:CFP). These results showed that the maximum crossover ratio is 0.11 of GFP filter set in CFP-accumulating nuclei, meaning that we can expect to detect CFP signals in the nuclei using our GFP filter set with approximately 10% of the intensity of CFP signals using the proper (CFP) filter set. On the other hand, we can expect to see no crossover signals with EYFP-expressing samples after removing background. Therefore, we should be able to distinguish each nucleus based on the crossover ratio (the profiles) in a single viewing frame where nuclei accumulate different fluorescent proteins.

To demonstrate the feasibility of this method, we infiltrated four different *A. tumefaciens* strains that carry different binary vectors (expressing ECFP, ELGFP6.1, EYFP, or DsRed2 fused to TGA5) in the same area on a tobacco leaf. When older (plants in reproductive phase) tobacco plants were used, the transformation efficiency of mesophyll cells decreases and many of the cells were transformed with a single *A. tumefaciens* strain (N. Kato and E. Lam, unpublished data). After we inoculated the four different *A. tumefaciens* strains into the leaves of older plants, images were captured using filter sets optimized for the four fluorescent proteins and we analyzed the fluorescence emission intensity ratios for each nucleus as described above. The steps taken to spectrally resolve the origin of nuclear fluorescence from the four distinct fusion proteins in a single viewing field are described in Figure 5. First, we captured the images using filter sets optimized for the four fluorescent proteins. Non-background-subtracted images with each filter set are aligned in Figure 5A. Based on each of these images alone, we cannot assign unambiguously the origin for each fluorescence signals from each nucleus due to crossover of fluorescence. Second, we subtracted the background signals that are obtained from the mock-treated area in the same leaf (Fig. 5B). Third, we analyzed the crossover profiles in each nucleus area as well as non-nucleus area. Each nucleus that is marked by a red circle with numbers from 1 to 4 in Figure 5C showed a ratio of 0:0:0.07:1, 1:0.07:0:0, 0:0.03:1:0.02, and 0.06:1:0.03:0.01 (RD:YFP:GFP:CFP),

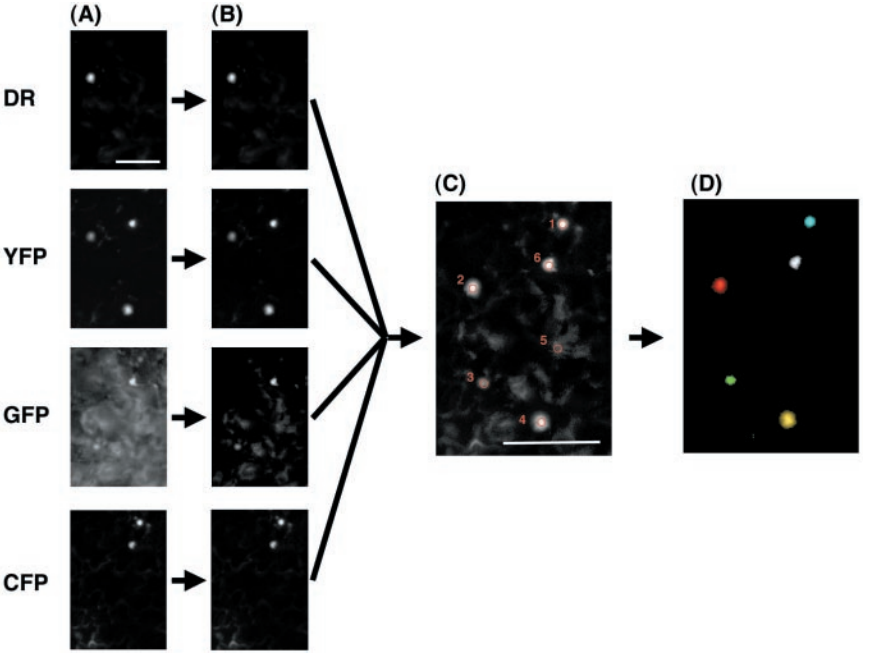

Figure 5. Multicolor observation in a single viewing frame and the imaging procedure. Nuclei accumulating DsRed2, EYFP, ELGFP6, or ECFP in a same area of mesophyll cells of a tobacco leaf were observed. A, Non-background-subtracted images with each filter set are shown. DR, YFP, GFP, and CFP show the particular filter set that was used. B, Background-subtracted images from each filter set. C, Superimposed image from B. The red circles with the numbers indicate the area where the crossover profiles are made. The ratios of RD:YFP:GFP:CFP in each area are shown here. Area 1, 0:0:0.07:1; area 2, 1:0.07:0:0; area 3, 0:0.03:1:0.02; area 4, 0.06:1:0.03:0.01; area 5, 1:0.06:0.89:0.08; area 6, 0:1:0.56:0.44. The images of each nucleus were colored based on the profiles. Red, DsRed2; yellow, EYFP; green, ELGFP6.1; cyan, ECFP; white, co-accumulated nucleus as white. Bar = 50 μm.

respectively. Each ratio matches to one of the fluorescence protein profiles described above. Meanwhile, the non-nucleus area marked as number 5 in Figure 5C shows the ratio of 1:0.06:0.89:0.08 (RD:YFP:GFP:CFP), which does not resemble any of the fluorescence profiles for the four proteins. Therefore, we can distinguish and properly assign each fluorescence protein to the signals in the image based on the spectral profiles. The nucleus marked as number 6 shows the ratio of 0:1:0.56:0.44 (RD:YFP:GFP:CFP). This indicates that EYFP, ELGFP6.1, and ECFP proteins may be co-accumulated in the single nucleus though we cannot predict the mix ratio of the three proteins. We also cannot remove the possibility that very low levels of the other fluorescent proteins may be present in the nucleus where typical profiles were obtained for one of the proteins. The final background-subtracted composite image from overlaying the four images obtained with the different filter sets is shown in Figure 5D. Each nucleus is colored based on the profiles and image objects whose intensity profiles do not match to any of the four fluorescence proteins were removed. The co-accumulated nucleus is shown in white. From this demonstration, we concluded that one can readily distinguish each of the four different fluorescent proteins from each other in the same viewing field. We have to emphasize that one cannot easily distinguish the four fluorescent proteins with this method in cases where the nuclei contain very low amounts of fluorescent proteins with signal levels that are near or below the background, or more than two colocalized fluorescent proteins with drastically different accumulation levels. In these cases, much more sophisticated methods such as fluorescence lifetime microscopy at a pixel-by-pixel scale would be necessary to more accurately assign and quantitate the various fluorescent proteins in the tissues of concern.

Detection of Protein-Protein Interactions in Tobacco Leaf Nuclei by FRET

We combined the simple transient transformation method and the imaging methodology described above to detect protein-protein interactions of a transcription factor in a single nucleus. We studied the dimerization of TGA transcription factors in plants using EYFP- and ECFP-tagged fusion proteins. The basic Leu zipper DNA-binding domain of TGA is known to form dimers in a parallel orientation. For our test case, we fused Arabidopsis TGA5 to the 3′ end of GFP variants. Figure 6A shows that DAPI staining signals overlapped with GFP signals, thus confirming the expression of these fusion proteins is exclusively nuclear. We then mixed two *A. tumefaciens* strains that carry vectors expressing EYFP or ELGFP6.1 fusion proteins, and co-infiltrated them together into tobacco leaf tissues. Three different fluorescence patterns in nuclei of the infiltrated areas could be observed after removing the background signals from the image as described before (Fig. 6B). In the viewing field that we present in this figure, two nuclei were detected with the YFP filter set. With the GFP filter set, two fluorescent nuclei were also observed with only one of these also detected with the YFP filter set. Thus, this nucleus must be co-expressing both ELGFP6.1 as well as EYFP. This result demonstrated our ability to distinguish three different expression patterns by co-infiltration with two *A. tumefaciens* strains. In two nuclei, one of two T-DNAs was transferred and expressed, whereas in the third nucleus, both T-DNAs were transferred and

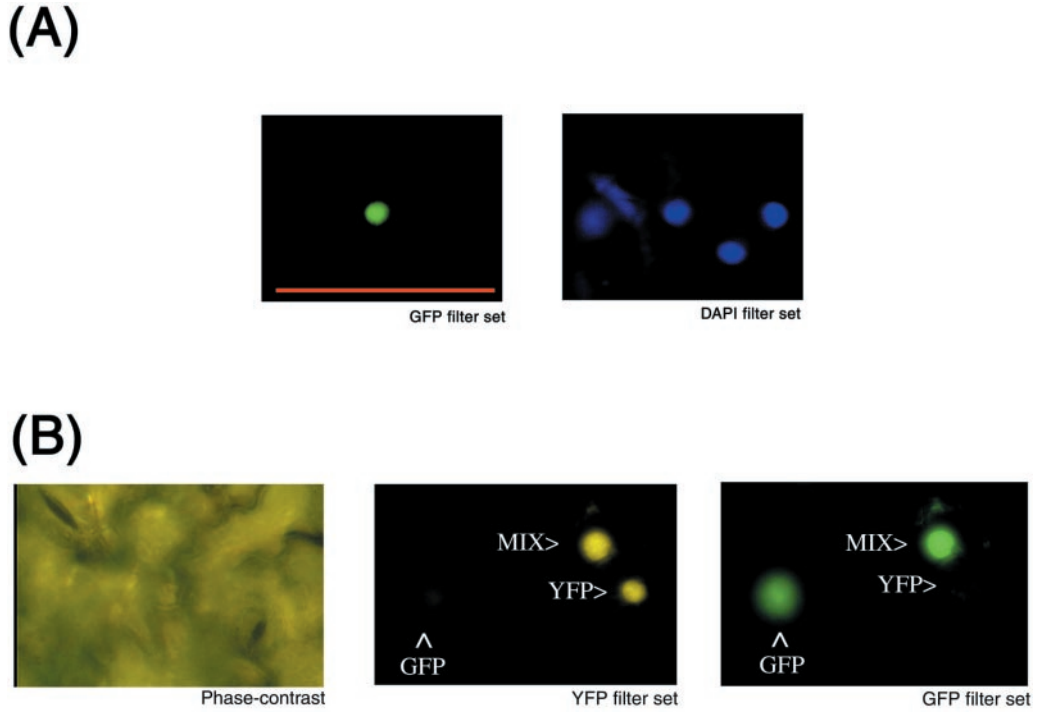

Figure 6. Dual T-DNA transformation using the *A. tumefaciens* filtration method confirmed by EYFP and ELGFP6.1 dual expression. A, Tobacco leaf infiltrated with *A. tumefaciens* expressed ELGFP6.1 protein in nuclei. Fluorescent microscopy with GFP filter set (left) or with 4,6-diamidino-2-phenylindole (DAPI) filter set (right). Bar = 50 μm. B, Tobacco leaf infiltrated with two different *A. tumefaciens*, expressing ELGFP6.1 and EYFP in nuclei. Observation with phase contrast (left), YFP filter set (middle), or GFP filter set (right). GFP> and YFP> indicate nuclei showing green fluorescence or yellow fluorescence, respectively. Mix> indicates dual detection of green and yellow fluorescence from a single nucleus.

expressed. Our study also shows clearly that multiple T-DNAs from different *A. tumefaciens* can be simultaneously transferred and expressed in a single plant cell using this transient expression system. This is consistent with previous studies involving stable transformation by *A. tumefaciens* strains, which indicated multiple T-DNAs can be transferred to a single plant cell (Depicker et al., 1985).

Taking advantage of the ability to express and resolve different fluorescent proteins with our method, we performed FRET analysis to detect protein-protein interactions between transcription factors in planta. FRET is a phenomenon whereby a fluorescent molecule (the donor) transfers energy efficiently to a neighboring chromophore (the acceptor) when the emission spectrum of the donor significantly overlaps with the excitation spectrum of the acceptor. This type of energy transfer is highly dependent on the physical distance between the two interacting molecules and the two chromophores need to be located within 10 to 100 Å of each other for significant FRET to occur (Gadella et al., 1999). For example, in FRET using the CFP-YFP pair, cyan fluorescence emission from CFP is decreased when the interacting molecules are excited by actinic light for CFP with concomitant observation of fluorescence from the acceptor YFP partner. Thus, FRET can be measured by the change in donor/acceptor fluorescence emission ratios. FRET using CFP and YFP has been applied in animal and plant cells (Miyawaki et al., 1997; Gadella et al., 1999) to monitor calcium by using a "chameleon" protein in which calmodulin and a calmodulin-binding peptide M13 was inserted between CFP and YFP. In the presence of calcium, the intramolecular interaction between calmodulin and M13 brings CFP and YFP close to each other enough for FRET to occur. Using FRET between BFP and GFP fused to Bcl2 and Bax, it has also been shown that two different proteins that are related to apoptosis can interact on the mitochondrial membrane of animal cells in vivo (Mahajan et al., 1998). More recently, Mas et al. (2000) showed evidence for GFP-DsRed FRET in plant protoplasts.

Gadella et al. (1999) pointed out the complexity of FRET analysis in plants: (a) Donor/acceptor fluorescence intensity ratio also depends on microscope optics and the relative local concentrations of donor and acceptor molecules, and (b) Existence of fluorescence absorption factors such as chlorophyll pigments in plants can decrease the apparent fluorescence intensity in the observed cells and can cause misinterpretation of FRET (Gadella et al., 1999). Thus, several different methods have been used to analyze FRET with a microscope (Miyawaki et al., 1997; Mahajan et al., 1998; Gadella et al., 1999; Mas et al., 2000). We adapted the simpler approach of using a set of con-

trol experiments for detecting FRET and normalize for background (Miyawaki et al., 1997). As a negative control, EYFP-LexA/nuclear localization signal (NLS) was co-expressed with ECFP-TGA5. EYFP-LexA/NLS will accumulate in the nucleus of plant cells because it carries the SV40 T-antigen NLS, but it is not expected to form dimers with TGA5. In this case, no FRET would be expected to occur even though both proteins will be expressed in the same nucleus simultaneously. This negative control also allows us to compensate for the complex factors of FRET analysis mentioned above.

The infiltrated tobacco leaves were observed at 4 d after infiltration using different excitation and emission filter combinations. To detect FRET, the ratio of cyan (470/30 nm) to yellow (535/30 nm) fluorescence emission under CFP excitation (436/10 nm) was measured for each nucleus examined. In each case, the fluorescence of CFP and YFP emission with CFP and YFP excitation, respectively, was also measured. When FRET occurs, the apparent quantum yield for a constant amount of CFP (measured by EX_{CFP}:EM_{CFP}) will decrease because some of the CFP emission will be converted to YFP. On the other hand, the apparent quantum yield for YFP (EX_{YFP}:EM_{YFP}) should essentially be constant. In the nuclei where only ECFP-TGA5 or EYFP-TGA5 genes was expressed, homodimers of these fusion proteins will be expressed in nuclei of the infiltrated tissues. In tissues where both ECFP-TGA5 and EYFP-TGA5 were expressed, the two different TGA5 fusion proteins would form homo- and heterodimers, and the ratio of the yellow emission to cyan emission under CFP excitation would increase due to FRET. In contrast, in nuclei where ECFP-TGA5 and EYFP-LexA/NLS were expressed, only homodimers would form and the ratio of yellow emission to cyan emission under CFP excitation should not increase.

One of the key factors to be taken into account to measure FRET accurately is to precisely measure the amount of background fluorescence (Periasamy and Day, 1999; Sorkin et al., 2000). Background signals can be determined accurately by measuring the intensities in the same viewing areas after photobleaching (Sorkin et al., 2000). Photobleaching can be performed by continuous excitation through CFP and YFP filter sets. In animal cells, this does not cause any detectable morphological changes as well as fading of cell autofluorescence. In our conditions, however, photobleaching with the CFP filter set causes morphological changes of nuclei (data not shown). Therefore, it is very difficult to perform photobleaching with plant tissues without causing drastic perturbations to cellular structures. We found that the fluorescence intensities obtained from nuclei that do not accumulate fluorescent proteins are nearly the same as those of areas in the cytosol that do not contain chloroplast (data not shown). Therefore, as an alternative to photobleaching, we measured signals from the cytosolic areas of the cells that are accumulating fluorescent proteins in their nuclei to obtain the accurate background signals. This is different from the background measurement performed in Figures 2, 3, and 5, where the signals in the entire viewing field are averaged out. The nuclear signals used for FRET analysis were subtracted by the background signals obtained from the cytosol areas to generate more precise corrected fluorescence values.

To verify that these proteins can be expressed to similar levels, we performed western-blot analysis using anti-GFP polyclonal antibodies on the same samples that were used for microscopy (Fig. 7). The apparent size for ECFP-TGA5 and EYFP-TGA5 was detected at approximately 78 kD on the blot. Two cross-reacting peptides at 54 and 50 kD were also observed in some of our samples and may be proteolysis products. EYFP-LexA/NLS was detected at approximately 40 kD. Dual infiltrated samples of ECFP-TGA5 and EYFP-LexA/NLS showed two distinct bands at the predicted size, whereas Coomassie Brilliant Blue-stained gels showed similar amounts of proteins are loaded onto each lane. These results suggest that the proteins can be expressed to similar levels under our conditions. This is confirmed by measuring the amount of EYFP fluorescence in each of the infiltrated samples using the EYFP-specific filter set. Figure 8A shows quantitation of EYFP fluorescence (500/20 nm excitation and 535/30 nm emission) per pixel after subtraction of the background signals from individual nucleus of each infiltrated tissue sample. The data suggest that the averages of

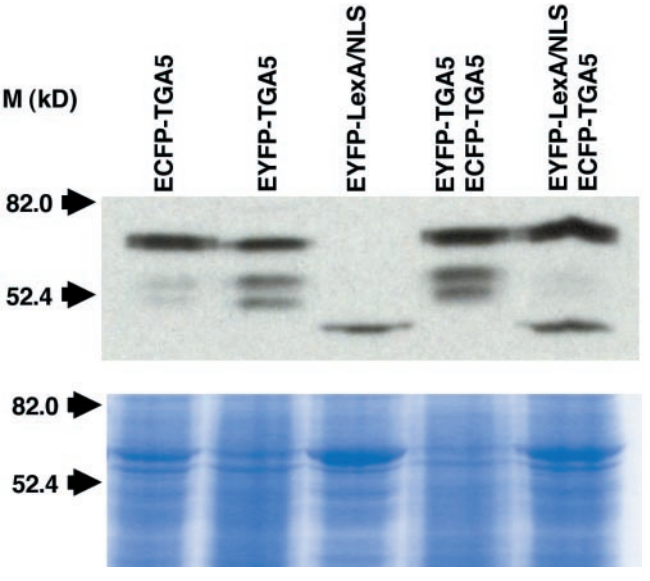

Figure 7. Western-blot analysis of dual-infiltrated tobacco leaves. Tobacco leaves used for FRET analysis were analyzed. Upper, Blotted membrane against polyclonal anti-GFP antibodies. Lower, Coomassie Brilliant Blue dye-stained SDS polyacrylamide gel where similar amounts of proteins as for western blot were loaded. Arrows indicate the positions for protein markers with the sizes indicated in kD. M, Protein markers.

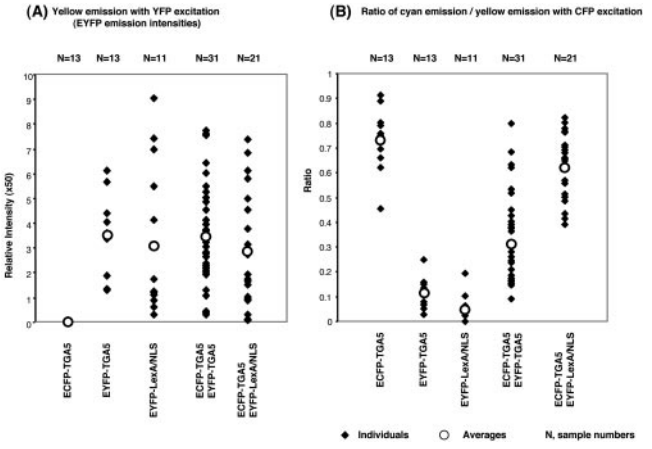

Figure 8. FRET analysis in tobacco leaf nuclei. A, EYFP emission intensities in each nucleus. Black diamonds show the EYFP fluorescence (535/30 nm emission and 500/20 nm excitation) intensities per pixel in each nucleus. White circles show the average values observed for each infiltrated sample. *n* = sample numbers. B, Ratio of cyan emission (470/30 nm) to yellow emission (535/30 nm) at CFP excitation (436/10 nm). Cyan emission (470/30 nm) intensity was divided by yellow emission (535/30 nm) intensity at CFP excitation (436/10 nm). Black diamonds show each ratio in nuclei observed with the different infiltration conditions. White circles show the average for each set of data.

the intensities for each sample infiltrated with constructs expressing EYFP fusion proteins were not significantly different ($P = 0.02$ in Student's t test for EYFP-TGA5- and ECFP-TGA5-co-expressing nuclei against EYFP-LexA/NLS- and ECFP-TGA5-co-expressing nuclei). This result is consistent with that of western-blot analysis shown in Figure 7.

To detect FRET, we calculated the ratio of cyan emission to yellow emission under ECFP excitation (cyan/yellow). In this calculation, cyan/yellow emission ratio should be high in ECFP-TGA5 expressing nuclei and should be low in EYFP-TGA5-expressing nuclei. Because the emission spectrum of CFP is rather broad, there is significant crossover with the emission spectrum of YFP. More importantly, the CCD camera we have with our system is much more sensitive in the yellow region of the spectrum than the blue; thus, when excited with actinic light in the region of optimum CFP excitation, there is actually more apparent fluorescence observed with the YFP emission filter than with the CFP emission filter when raw data are compared. This explains the average value of about 0.75 observed for the CFP/YFP emission ratio in the absence of expressed YFP. In EYFP-TGA5-expressing nuclei, the mean of cyan/yellow emission under cyan excitation was 0.110, which suggests that EYFP is not excited appreciably by light from the CFP excitation filter. When we co-expressed ECFP-TGA5 and EYFP-TGA5, the cyan/yellow ratio of co-expressing nuclei (average = 0.331) was significantly lower ($P < 0.0001$ in Student's t test). In contrast, the cyan/yellow emission ratio in ECFP-TGA5- and EYFP-LexA/NLS-co-expressing nuclei (average = 0.627) was not significantly different ($P = 0.022$ in Student's t test) from that of ECFP-TGA5-expressing nuclei. These data indicate that FRET was occurring between the ECFP-TGA5 and EYFP-TGA5 heterodimers, whereas no significant FRET is detected with ECFP-TGA5 and EYFP-LexA/NLS expression.

In conclusion, these results demonstrated that protein-protein interactions between transcription factors can be monitored in planta using live tissues. The combination of FRET with transient expression via *A. tumefaciens* represents a rapid and facile method to detect protein-protein interactions of transcription factors in living plant cells in addition to more invasive techniques such as immunoprecipitation. We showed the feasibility of multicolor observation in tobacco leaves using a typical transcription factor, TGA5, which specifically accumulates in the nucleus, a subcellular compartment that has low autofluorescence. Although this particular model system may not be representative of all subcellular compartments for all cells in a plant, we note that our novel approach of using spectral profiling in combination with digital imaging and background subtraction allowed the detection of up to four distinct fluorescent proteins that have overlapping spectral properties in a single viewing frame with leaf tissues. Thus, this work demonstrated the feasibility of using these autofluorescent proteins to simultaneously track multiple proteins in different locations within a plant cell. In addition, further optimization of the methods and tools developed in this study should open up the possibility of studying multiple protein-protein interactions in organelles other than nuclei in plant cells, such as mitochondria and plastids.

MATERIALS AND METHODS

Gene Constructs

Primers EL768 (5′-GGATCCTCTAGAATGAGTAAAGGAGAA-3′) and EL769 (5′-GAGCTCAGATCTTTTGTATAGTTCATC-3′) were used to remove the endoplasmic reticulum retention signal from mGFP5-ER (Haseloff, 1999) by PCR. The resultant PCR product contains *Bam*HI and *Xba*I sites located before the initiation codon and *Bgl*II and *Sst*I sites after the last amino acid residue (Leu) in mGFP5. The cycle conditions were 94°C for 1 min, 52°C for 1 min, and 72°C for 40 s, with a total of 35 cycles. The PCR product was subcloned into *Eco*RV-digested pBluescript II SK (−) plasmid (Stratagene, La Jolla, CA) and completely sequenced. The clone was designated pmGFP5-SK. *Bam*HI- and *Sal*I-digested mGFP5 fragment from pmGFP5-SK was subcloned in *Bam*HI- and *Sal*I-digested pET23a vector (Novagen, Madison, WI) and designated pET23a-mGFP5. To create ELGFP6, which has a Ser-65 to Cys mutation in mGFP5, primers EL853 (5′-TGTCACTACTTTCTGTTATGGTGTTCA-3′) and EL769 were used for the PCR. The eluted PCR product and primer EL768 were used to create full-length ELGFP6 by a second round of PCR. The PCR conditions were the same as above. The PCR product was then subcloned into *Eco*RV-digested pBluescript II SK (−) plasmid and completely sequenced. The clone was designated as pELGFP6-SK. pELGFP6-SK was used as a template to create ELGFP6.1 with Phe-64 converted to Leu by PCR amplification with primers EL768 and EL882 (5′-ACAAAGTAGTGACAAGTGTT GG-3′). The PCR product and primer EL769 were used to create full-length ELGFP6.1. The PCR product was then subcloned into *Eco*RV-digested pBluescript II SK (−) plasmid and completely sequenced. The clone was designated as pELGFP6.1-SK.

The EYFP-coding region of pEYFP-C1 plasmid (CLONTECH Laboratories) was amplified with primers EL874 (5′-GGATCCTCTAGAATGGTGAGCAAGGGC-3′) and EL875 (5′-GAGCTCAGATCTCTTGTACAGCTCGTC-3′), which create *Bam*HI and *Xba*I sites before the initiation codon and *Bgl*II and *Sst*I sites after the last amino acid residue. The PCR product was subcloned and sequenced to confirm as above. An *Hin*dIII- and *Eco*RI-digested fragment of pEG202 (Golemis and Brent, 1992) encoding bacterial LexA was cloned into *Hin*dIII- and *Bam*HI-digested pLacI/NLS-SK and the clone was named pLexA/NLS-SK. An *Not*I- and *Hin*dIII-digested fragment of pEYFP-SK was cloned into *Xho*I- and *Hin*dIII-digested pLexA/NLS-SK with an *Not*I/*Xho*I adapter and the clone was named pEYFP-LexA/NLS-SK. A *Bam*HI- and *Not*I-digested fragment from pEYFP-LexA/NLS-SK was cloned into *Bam*HI- and *Sst*I-digested pBI221 via a *Not*I/*Sst*I adapter and the clone was named pEYFP/LexA/NLS-BI221. A *Bam*HI- and *Eco*RI-digested fragment from pEYFP-LexA/NLS-BI221 was cloned into *Bam*HI- and *Eco*RI-digested pEL103 and the clone was designated pEYFP-LexA/NLS-EL103.

The ECFP-coding region of pECFP-C1 plasmid (CLONTECH Laboratories) was amplified with primers EL874 and EL910 (5′-GAGCTCAAGCTTCTTGTACAGCTCGTC-3′), which create *Bam*HI and *Xba*I sites before the initiation codon and *Hin*dIII and *Sst*I sites after the last amino acid residue (Lys). The PCR product was then subcloned and sequenced as above.

Arabidopsis TGA5 isolated from a meristem-enriched cDNA library was amplified using primers EL424 (5′-CGGATCCATGAGAAACATCAGTCTCAAC-3′) and EL426 (5′-CGTCGACTCAAGATCCTCTCTTGGTCTGGCAA-3′), which create a *Bam*HI site and initiation codon before the first amino acid residue (Arg) of the cDNA clone and *Bgl*II sites after the last amino acid residue (Glu). Fusion of the TGA5 sequence with those of EYFP and ECFP were carried out by appropriate subcloning strategies.

Spectroscopy

A model F-4500 fluorescence spectrophotometer (Hitachi Instruments, San Jose, CA) was used to measure the fluorescence spectra of mGFP5, ELGFP6, and ELGFP6.1 proteins, as well as to quantitate their relative fluorescence yield.

Agrobacterium tumefaciens Infiltration

A. tumefaciens strain GV3101/pMP90 was transformed according to Chen et al. (1994). A single colony of transformed *A. tumefaciens* was inoculated in 2 mL of Luria-Bertani broth containing 25 μg mL^{-1} gentamycin and 50 μg mL^{-1} kanamycin at 28°C overnight. Each culture was collected in a 2-mL tube and was centrifuged at 1,000 rpm for 5 min. Bacteria pellets were then resuspended in water to an optical density at 600 nm of about 0.5. The resuspended bacteria (1 mL) were inoculated into abaxial sides of 1- to 2-month-old tobacco (*Nicotiana tabacum*) leaves using a 1-mL syringe. Five to six infiltrations were performed with approximately 2-cm-diameter infiltration areas. When DAPI was inoculated, 1 mL of DAPI (0.2 μg mL^{-1} in water) was infiltrated 12 h after *A. tumefaciens* was infiltrated. The efficiency of cell transformation of mesophyll cells seems to highly depend on the growth phase of plants. In our condition, the efficiency drastically drops after the plants enter the reproductive phase (N. Kato and E. Lam, unpublished data). When four *A. tumefaciens* strains were inoculated for multicolor detection in a single viewing frame, 250 μL of each culture was mixed in a 2-mL tube before pelleting by centrifugation. The mixed solutions were then infiltrated into leaves of plants at the reproductive phase (4–5 months old). When FRET analysis was performed, 500 μL of each culture was mixed in a 2-mL tube before centrifugation. The solutions were then infiltrated into leaves of plants in the vegetative phase. The inoculated regions (approximately 2 × 2 cm) were dissected with scissors 4 d after the inoculation. The dissected discs were mounted on microscope slides with water and covered with a coverslip before observation.

Microscopy

A TE200 (Nikon, Tokyo) inverted microscope equipped with Nikon 60× numerical aperture (N.A.) 1.2 objective lens, Nikon 20× N.A. 0.75 objective lens, and 10× N.A. 0.25 objective lens. The images were captured with a cooled, 12-bit CCD camera, model CH350 (Photometrics, Tucson, AZ). All filters were purchased from Chroma Technology Corporation. The filters for EYFP (YFP filter set) were: exciter, 523/20 nm; emitter, 568/50 nm; and JP3 beamsplitter. Exciter 460/20 nm, emitter 500/22 nm, and JP3 beamsplitter were used for ELGFP6.1 (GFP filter set). Exciter 436/10 nm, emitter 470/30 nm, and JP4 beamsplitter were used for ECFP (CFP filter set). Exciter 380/30 nm, emitter 445/40 nm, and BFP/GFP beamsplitter were used for EBFP. Exciter 555/28 nm, emitter 617/73 nm, and 810 beamsplitter were used for DsRed2 (RD filter set). When FRET analysis was performed, exciter 500/20 nm, emitter 535/30 nm, and JP4 beamsplitter was used to observe the EYFP fluorescence. The JP4 beamsplitter was also used for FRET analysis.

Image Processing

The images were analyzed by softWoRx software (Applied Precision, Issaquah, WA) on an Octane Workstation (Silicon Graphics, Mountain View, CA). The images were processed by Adobe Photoshop 5.5 (Adobe Systems, Mountain View, CA) on a PowerMac G4 computer (Apple Computer, Cupertino, CA) for the final display. Some of the imaging data were transferred to Excel (Microsoft; Redmond, WA) for calculations.

Quantification of Background Signals in the Tobacco Leaves

One- to 2-month-old tobacco leaves were dissected and placed on the microscope stage supported by a glass slide with a coverslip. Distilled water was used as mounting medium, and abaxial side of the leaf was facing the objective lens. Fluorescent images were captured on a 256- × 256-pixel CCD camera with a 10× objective lens with 0.3-s exposure time. The filter sets were switched automatically without changing the viewing field. This resulted in creating five images (for RD, YFP, GFP, CFP, and BFP filter set) for the same area of observation. Three independent experiments were performed using three different plants. The sum of the intensity values for each filter set was then divided by the total pixel number to obtain the background value. The final background intensity values (MBs) were calculated by the following method: MB is the mean of B in three independent experiments; B = SI/P, where B = background intensity in each experiment, SI = sum of intensity values in the observed area, and P = total pixel numbers in the observed area (256 × 256).

Calculation of S/B of Fluorescent Proteins in Tobacco Mesophyll Cells

The infiltrated tobacco leaves were dissected out and then observed under conditions described above. Three independent experiments were performed using three different plants. The nucleus areas, which are clearly evident by their shape and size, were then selected from the images. The selected nuclei would contain at least 2 times higher signal values than that of background. The intensity values of each fluorescent protein in the observed nuclei were then subtracted by the background values that were obtained previously as described above. The background-subtracted values were then averaged per nucleus. Thus, the final signal-to-background ratios (MSBs) were calculated by the following method: MSB is the mean value of SB. Sample number (n) for ECFP is 57, EGFP6.1 is 65, EYFP is 100, and DsRed2 is 54.

$$SB=(IN-IB)/IB$$

where SB = S/B in a nucleus, IN = intensity values of a nucleus area, and IB = background intensity values of the same nucleus area = MB × pixel numbers of nucleus area.

Creating Images of Fluorescent Protein-Accumulating Nuclei

The mesophyll cell images which expressed one of the fluorescent protein were taken with a 60× objective lens. The filter sets were switched automatically without changing the viewing field to obtain the images with each filter set, which resulted in creating four images for each fluorescent protein.

The fluorescence intensities in a given image were recorded on the CCD with 12-bit (0–4,095) dynamic ranges. Under our conditions, the averages of noise signals are approximately 50 to 80 (Fig. 2). We set up shutter speeds and magnifications so that all fluorescence intensity values would be in

range (maximum 4,094). The resultant image data was then scaled from 12-bit data (0–4,095) to be displayed as 8-bit (0–255) gray level image due to limitation of our monitor and printer capability. For example, for image data intensities ranging from 0 to 1,000, the computer will convert the detected signals in the range of 0 to 1,000 to the display range of 0 to 255. If the minimum scale is 500 and the maximum is 3,000, all values 500 and below of the original data will be displayed as zero (black); all values 3,000 and above are displayed as 255 (white). To add color in the images, the images are saved as 8-bit gray scale TIFF images and then transferred to Adobe Photoshop. Therefore, the actual intensity data and the image may not be correlated in the resultant images.

Making Fluorescent Profiles in the Nucleus

The infiltrated areas of tobacco leaves were dissected out and then observed with a 10× objective lens. Three independent experiments were performed using three different plants. The filter sets were switched automatically without changing the viewing field to obtain the images for each filter set, which resulted in creating four images for each fluorescent protein. The background values of each filter set were then subtracted from each pixel of the images. The nucleus areas, which are judged by its shape using the image that was taken with the optimal filter set for the particular fluorescent protein (i.e. the images that were taken with RD filter set for DsRed2-expressed sample) were then selected. The selected nuclei would contain at least 2 times higher signal values than that of background. The same areas were selected in the images that were taken using the other filter sets (i.e. the images taken with YFP, GFP, and CFP filter set for DsRed2-expressed samples). If the resultant intensity became less than 0, we scaled its value to 0.

The intensity ratios for each nucleus area on the same viewing field with different filter sets were then calculated. The values obtained with the optimal filter set were scaled as 1. The resultant ratio was averaged per nucleus. Therefore, the final ratios (MRs) were calculated by the following method: MR is the mean of R (ECFP $n = 57$, EGFP6.1 $n = 65$, EYFP $n = 100$, and DsRed2 $n = 54$), and R = Q/S, where R = crossover ratio for a query filter combination in a nucleus, Q = background-subtracted intensity values for nucleus with a query filter set = IN − IB with a query filter set (if $Q < 0$, then $Q = 0$), and S = background-subtracted intensity values for nucleus with a proper filter set = (IN − IB) with the optimized filter set.

Multicolor Observation

The infiltrated leaves from tobacco in the reproductive phase were observed with a 20× objective lens with each filter set without changing the field of viewing. The R values for each filter set were calculated for each nucleus.

FRET Analysis

A. tumefaciens carrying the binary vector expressing ECFP-TGA5, EYFP-TGA5, or EYFP-LexA/NLS was used to infiltrate tobacco leaves. Five different combinations of infiltrations were performed (ECFP-TGA5 alone, EYFP-TGA5 alone, ETFP-LexA/NLS alone, ECFP-TGA5 and EYFP-TGA5 mix, and ECFP-TGA5 and EYFP-LexA/NLS mix). The abaxial sides of the infiltrated tobacco leaves were observed with a 60× objective lens. When two different proteins were expressed in the same sample, the nuclei expressing both ECFP and EYFP were identified by switching the YFP and CFP filter set. The nuclei detected by both filters were selected. The cell images were taken with three different filter sets (emission filter:excitation filter = 470/30:436/10 nm, 535/30:500/20 nm, and 535/30:436/10 nm) by switching the excitation and emission filters, which resulted in creating three images for one nucleus.

The same areas in the nucleus were selected from each image for FRET analysis. Background values were obtained from cytosolic areas of the same cells for each filter set. The averaged values of background signals (per pixel) were used to subtract the background from the selected nucleus area. The background-subtracted values for each filter set were then recorded. The ratio of cyan (470/30 nm) to yellow (535/30 nm) fluorescence emission under CFP excitation (436/10 nm) was measured for individual nuclei. In each case, the fluorescence of CFP and YFP emission with CFP and YFP excitation respectively was also measured. The EYFP emission intensities and the ratios of cyan to yellow fluorescence emission under CFP excitation were then subjected to Student's *t* test to determine the *P* value. Thus, FRET was measured in our samples by the following method: Dy, YFP emission (500/20 nm ex, 535/30 em) intensity of a nucleus where only donor proteins (ECFP-TGA5) are expressed; Ay, YFP emission intensity of a nucleus where only acceptor proteins (EYFP-TGA5) are expressed; Ny, YFP emission intensity of a nucleus where only negative control of acceptor proteins (EYFP-LexA/NLS) are expressed; DAy, YFP emission intensity of a nucleus where both donor and acceptor proteins are expressed; DNy, YFP emission intensity of a nucleus where both acceptor and negative control proteins are expressed; Dc, CFP emission (436/10 nm ex, 470/30 em) intensity of a nucleus where only donor proteins are expressed; Ac, CFP emission intensity from a nucleus where only acceptor proteins are expressed; Nc, CFP emission intensity of a nucleus where only negative control for acceptor proteins are expressed; DAc, CFP emission intensity of a nucleus where both donor and acceptor proteins are expressed together. DNc, CFP emission intensity of a nucleus where both donor and negative control proteins are expressed together; Df, FRET emission (436/10 nm ex, 535/30 em) intensity of a nucleus where only donor proteins are expressed; Af, FRET emission intensity of a nucleus where only acceptor proteins are expressed; Nf, FRET emission intensity of a nucleus where only negative control of acceptor proteins are expressed; DAf, FRET emission intensity of a nucleus where both donor and acceptor proteins are expressed; and DNf, FRET emission intensity of a nucleus where both acceptor and negative control proteins are expressed.

Background signals in each filter condition are measured from an area of the cytosol in the same cell. Averaged values for the signal per pixel were multiplied by the pixel number in each nucleus studied. The resultant values were used as background values for each nucleus examined and the values shown were those obtained after background subtraction. For each nucleus examined, values of Dy ($n = 13$), Ay ($n = 13$), Ny ($n = 11$), DAy ($n = 31$), and DNy ($n = 21$) were plotted. Dy was used to confirm that little or no crossover of donor fluorescent proteins. Ay, Ny, DAy, and DNy were used to confirm similar levels of protein accumulations by Student's *t* test. Dc/Df ($n = 13$), Ac/Af ($n = 13$), Nc/Nf ($n = 11$), DAc/DAf ($n = 31$), and DNc/DNf ($n = 21$) were calculated and plotted. Dc/Df, Ac/Af, and Nc/Nf were used to confirm the crossover ratio of FRET filter combination. Dc/Df, DAc/DAf, and DNc/DNf were used to test FRET phenomenon by Student's *t* test. If the result of Student's *t* test with Dc/Df and DNc/DNf showed no significant difference and the result of Student's *t* test with DAc/DAf and DNc/DNf showed a significant difference, it would suggest the existence of FRET between donor and acceptor proteins. Because each nucleus may accumulate different amount of donor and acceptor proteins, statistical analysis of data collected for a large number of individual nuclei are required.

Western-Blot Analysis

Leaf tissues (2- × 2-cm discs) after observation were collected in 2-mL tubes and submerged in liquid nitrogen. The frozen samples were stored at −80°C. To extract proteins for analysis, the frozen samples were ground in liquid nitrogen with the extraction buffer (150 μL of 6 M urea, 10%[w/v] glycerol, 10% [v/v] β-mercaptoethanol, and 5% [w/v] SDS) added immediately to the samples afterward. After 5 min of incubation on ice, the mixtures were then centrifuged at 14,000 rpm for 3 min to remove insoluble material. Ten microliters of non-heated supernatant was then used for western-blot analysis and Coomassie Brilliant Blue staining after SDS-PAGE. Anti-GFP polyclonal antibodies (CLONTECH Laboratories) were used at 1:5,000 (w/v) dilution to detect the proteins. Protein amounts in each sample were qualitatively compared with Coomassie Brilliant Blue dye staining SDS-polyacrylamide gel (Sambrook et al., 1989).

ACKNOWLEDGMENT

We thank Jim Haseloff for the mGFP5-ER construct.

Received March 13, 2002; returned for revision April 1, 2002; accepted April 11, 2002.

LITERATURE CITED

Chen H, Nelson RS, Sherwood JL (1994) Enhanced recovery of transformants of *Agrobacterium tumefaciens* after freeze-thaw transformation and drug selection. Biotechniques **16:** 664–669

Depicker A, Herman L, Jacobs A, Schell J, Van Montagu M (1985) Frequencies of simultaneous transformation with different T-DNAs and their relevance to the *Agrobacterium*/plant cell interaction. Mol Gen Genet **201:** 477–484

Gadella TWJ, van der Krogt GNM, Bisseling T (1999) GFP-based FRET microscopy in living plant cells. Trends Plant Sci. **4:** 287–291

Golemis EA, Brent R (1992) Fused protein domains inhibit DNA binding by LexA. Mol Cell Biol **12:** 3006–30014

Goodwin PC (1999) GFP biofluorescence: imaging gene expression and protein dynamics in living cells. Design considerations for a fluorescence imaging laboratory. Methods Cell Biol **58:** 343–367

Haseloff J (1999) GFP variants for multispectral imaging of living cells. Methods Cell Biol **58:** 139–151

Haseloff J, Siemering KR, Prasher DC, Hodge S (1997) Removal of a cryptic intron and subcellular localization of green fluorescent protein are required to mark transgenic Arabidopsis plants brightly. Proc Natl Acad Sci USA **94:** 2122–2127

Ikawa M, Yamada S, Nakanishi T, Okabe M (1999) Green fluorescent protein (GFP) as a vital marker in mammals. Curr Top Dev Biol **44:** 1–20

Johnson GA, Mantha SV, Day TA (2000) A spectrofluorometric survey of UV-induced blue-green fluorescence in foliage of 35 species. J Plant Physiol **156:** 242–252

Mahajan NP, Linder K, Berry G, Gordon GW, Heim R, Herman B (1998) Bcl-2 and Bax interactions in mitochondria probed with green fluorescent protein and fluorescence resonance energy transfer. Nat Biotechnol **16:** 547–552

Mas P, Devlin PF, Panda S, Kay SA (2000) Functional interaction of phytochrome B and cryptochrome 2. Nature **408:** 207–211

Miao ZH, Liu XJ, Lam E (1994) Tga3 Is a Distinct Member of the Tga family of Bzip transcription factors in *Arabidopsis thaliana*. Plant Mol Biol **25:** 1–11

Mittler R, Shulaev V, Lam E (1995) Coordinated activation of programmed cell death and defense mechanisms in transgenic tobacco plants expressing a bacterial proton pump. Plant Cell **7:** 29–42

Miyawaki A, Llopis J, Heim R, McCaffery JM, Adams JA, Ikura M, Tsien RY (1997) Fluorescent indicators for $Ca2^{+}$ based on green fluorescent proteins and calmodulin. Nature **388:** 882–887

Pepperkok R, Squire A, Geley S, Bastiaens PI (1999) Simultaneous detection of multiple green fluorescent proteins in live cells by fluorescence lifetime imaging microscopy. Curr Biol **9:** 269–272

Periasamy A, Day RN (1999) Visualizing protein interactions in living cells using digitized GFP imaging and FRET microscopy. Methods Cell Biol **58:** 293–314

Sambrook J, Fritsch EF, Maniatis T (1989) Molecular Cloning: A Laboratory Manual. Cold Spring Harbor Laboratory Press, Cold Spring Harbor

Smith H (2000) Phytochromes and light signal perception by plants: an emerging synthesis. Nature **407:** 585–591

Sorkin A, McClure M, Huang FT, Carter R (2000) Interaction of EGF receptor and Grb2 in living cells visualized by fluorescence resonance energy transfer (FRET) microscopy. Curr Biol **10:** 1395–1398

Stauber RH, Horie K, Carney P, Hudson EA, Tarasova NI, Gaitanaris GA, Pavlakis GN (1998) Development and applications of enhanced green fluorescent protein mutants. Biotechniques **24:** 462–466

Yang YN, Li RG, Qi M (2000) In vivo analysis of plant promoters and transcription factors by agroinfiltration of tobacco leaves. Plant J **22:** 543–551